APPLIED PHYSICS LETTERS **94**, 011903 (2009)

The use of nanocavities for the fabrication of ultrathin buried oxide layers

Xin Ou,[1,a] Reinhard Kögler,[1] Arndt Mücklich,[1] Wolfgang Skorupa,[1] Wolfhard Möller,[1] Xi Wang,[2] and Lasse Vines[3]
[1]*Forschungszentrum Rossendorf, PF 510119, D-01314 Dresden, Germany*
[2]*Shanghai Institute of Microsystem and Information Technology, Chinese Academy of Sciences, Shanghai 20050, People's Republic of China*
[3]*Department of Physics, University of Oslo, POB 1048 Blindern, 0316 Oslo, Norway*

(Received 6 November 2008; accepted 15 December 2008; published online 6 January 2009)

A continuous buried oxide layer with a thickness of only 58 nm is formed in silicon by oxygen implantation at 185 keV with a very low ion fluence of 1×10^{17} cm^{-2} and subsequent He implantation. Due to the implanted He efficient oxygen gettering occurs at the implantation induced damage and results in the accumulation of the implanted oxygen as well as of oxygen indiffused from the annealing atmosphere. The morphology and the resistivity of the resulting silicon-on-insulator structure are analyzed by cross section transmission electron microscopy and by cross section scanning spreading resistance microscopy. © *2009 American Institute of Physics*. [DOI: 10.1063/1.3065478]

Point defects in silicon induced by ion implantation have been widely investigated with regard to doping in silicon device processing.[1,2] The forward momentum transfer from the implanted ions to the silicon atoms in the collision cascades results in the presence of two distinct layers of vacancy excess close to the surface and interstitial excess at larger depth.[3–6] These implantation induced excess defects may act as gettering centers for, e.g., impurities.[7,8] Excess vacancy defects induced by oxygen implantation also serve as trapping centers for the implanted atoms by acting as nucleation sites for SiO_2 precipitation. The empty volume generated in the vacancy excess region assists the growth of the precipitates by balancing their volume expansion (by about 120%).[9,10] This mechanism is employed in this study for ion beam synthesis of a buried oxide (BOX) layer in Si, which is commonly known as the separation-by-implanted-oxygen (SIMOX) process. In SIMOX, silicon-on-insulator (SOI) substrates are fabricated by high-fluence oxygen implantation at elevated temperature and subsequent high temperature annealing.[11] Most of the oxide precipitates formed during SIMOX processing are distributed around the mean projected ion range (R_p) where the oxygen concentration reaches its maximum. However, many large SiO_2 precipitates are also formed at a shallower depth position around the damage maximum (D_p) of about $0.8R_p$, where the change is from the vacancy rich region to the interstitial rich one.[12–14] This is a problem especially for the low-fluence SIMOX processing (at fluences well below the stoichiometric limit) as a discontinuous oxide layer forms consisting of isolated precipitates. In order to create a homogeneous continuous BOX layer, the accumulation of the implanted oxygen in only one narrow layer is essential.[9] This shrinking of the BOX layer thickness in the SOI structure is required in order to enable downscaling of the SOI complementary metal-oxide-semiconductor architecture at suppressed short channel effect[15] and in order to improve the thermal conductivity.[16]

Also implanted He is known to be trapped mainly by vacancy defects to form a He-filled bubble layer at the position of the vacancy dominated layer.[17–20] Such a layer of He bubbles or of empty cavities (after He outdiffusing during high temperature annealing[17]) is efficient for gettering of implanted oxygen into a narrow layer[21] and also for gettering of oxygen indiffused from the annealing atmosphere.[22] In our study, a subsequent helium implantation is employed after the oxygen implantation to stabilize the excess vacancy defects formed during oxygen implantation by He-induced bubbles and to better define the depth of oxide seeding.

Czochralski-Si (100) wafers were implanted at 550 °C with 185 keV O^+ ions to a fluence of 1×10^{17} cm^{-2}. For this fluence, the maximum concentration of the as-implanted oxygen profile is only 10% of the oxygen concentration in stoichiometric SiO_2 (4.4×10^{22} cm^{-3}). Subsequently 45 keV He^+ ions were implanted at room temperature to fluences of 4×10^{16}, 8×10^{16}, and 2×10^{17} cm^{-2}. High temperature annealing was preformed at 1300 or 1350 °C for 3 h in an atmosphere containing Ar and O_2 at the ratio Ar/O_2 $=100/3$ or 100/30. In addition, a reference sample was fabricated by only oxygen implantation and subsequent annealing. The oxygen depth distribution was analyzed by means of secondary ion mass spectrometry (SIMS) using a Cameca IMS 7f instrument. The morphology and the resistance of the SOI structure were investigated by cross section transmission electron microscopy (XTEM) and cross section scanning spreading resistance microscopy (SSRM), respectively. For the cross section SSRM, the sample was cut manually and measured using a multimode atomic force microscopy (from Veeco instruments) equipped with a conductive Si tip coated with diamond.

Figure 1(a) presents the oxygen profiles obtained after the above processing. After annealing at 1300 °C, the oxygen profile of the reference sample shows only one peak located at the depth of 460 nm, which is close to R_p at 440 nm as calculated by the TRIM code.[23] For a low- and medium-fluence postimplantation of He, there are additional front peaks close to the depth of the calculated D_p position. The broadened R_p peak at lower He fluence may result from oxygen gettering at a certain amount of He, which is trapped by interstitial defects induced by the oxygen implantation,[20] which therefore cause the oxygen gettering there. As the He

[a]Electronic mail: x.ou@fzd.de.

 © 2009 American Institute of Physics

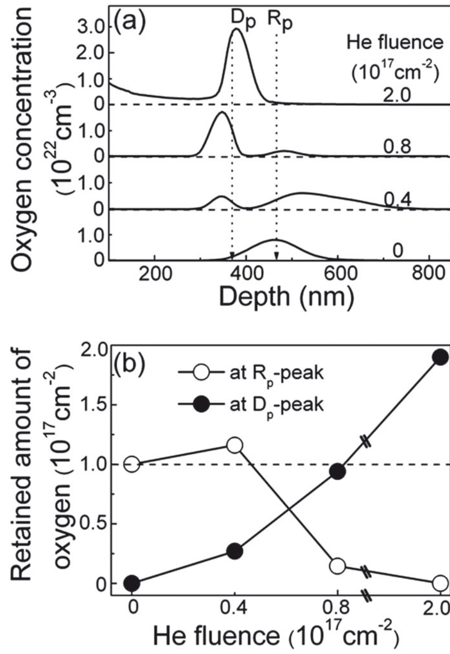

FIG. 1. (a) SIMS profiles of the oxygen distributions after postimplantation with He at different fluences and annealing at 1300 °C in 3% O_2 atmosphere for 3 h. The calculated positions of R_p and D_p are indicated. (b) Retained amount of the oxygen accumulated in the R_p peak and the D_p peak of the oxygen profiles vs He postimplantation fluence. The fluence of implanted oxygen is indicated by the dashed line.

fluence increases, more excess vacancies are generated in the vacancy rich region around D_p by the He implantation, in addition to those generated by the oxygen implantation. At the highest He fluence, all the oxygen is accumulated in the front peak at a depth of 370 nm. Figure 1(b) shows the retained amount of oxygen calculated by integrating the corresponding peaks of the profiles. The oxygen accumulation at the R_p region vanishes toward high He fluence, whereas the amount found around D_p even increases significantly above the implanted fluence. This indicates additional incorporation of oxygen by indiffusion from the annealing atmosphere. The corresponding XTEM image for the highest He fluence [Fig. 2(a)] shows a discontinuous BOX layer with a thickness of

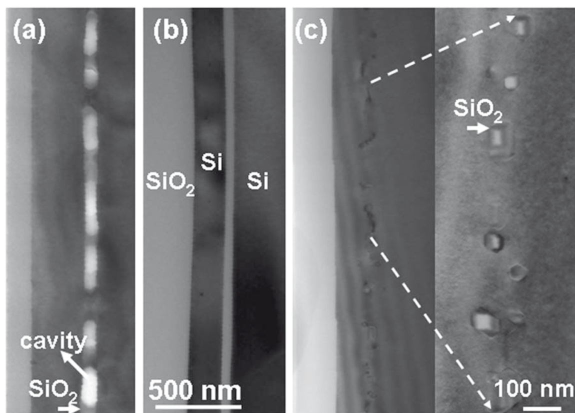

FIG. 2. Comparison of XTEM micrographs showing SOI structures formed by implantation of 185 keV ions to 1×10^{17} O cm^{-2}. (a) After 45 keV He postimplantation at 2×10^{17} cm^{-2} and annealing at 1300 °C in an atmosphere containing 3% O_2. The bright spots indicate cavities in the BOX layer. (b) Same, but after annealing at 1350 °C under 30% O_2, resulting in a continuous narrow BOX layer. (c) Reference sample annealed at 1350 °C in 30% O_2 showing widely distributed SiO_2 precipitates.

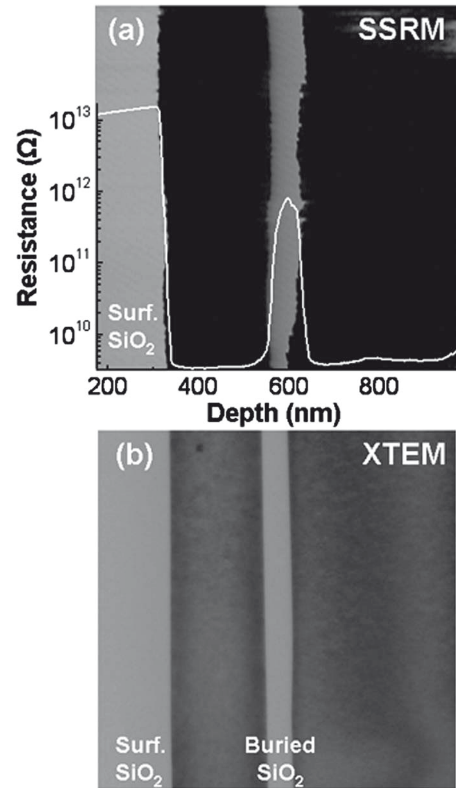

FIG. 3. (a) Cross section SSRM image of silicon implanted with 185 keV ions to 1×10^{17} O cm^{-2} plus 45 keV He ions to 2×10^{17} cm^{-2} and annealed at 1350 °C in 30% O_2. The dark and light colors indicate low and high resistance, respectively. A laterally averaged resistance scan curve is inserted. The scanning size is 0.8×0.8 μm^2. (b) Corresponding XTEM image with the same imaging area.

80 nm containing extended cavities (bright spots), which are similar to those recently reported by Ogura.[22] A continuous BOX layer [Fig. 2(b)] with a thickness of only 58 nm was achieved by enhanced oxygen indiffusion during annealing at increased temperature (1350 °C) and oxygen concentration (30%). Here, the total amount of retained oxygen of 2.6×10^{17} cm^{-2}, which is derived from the thickness of the BOX layer, exceeds the initially implanted fluence of 1×10^{17} cm^{-2} even more. Only few and disperse cavities remain in the BOX layer, and few dislocations in the top Si layer are observed by XTEM. The thickness of the BOX layer is not perfectly uniform, being slight larger at the positions of the remaining cavities. In comparison, a layer of isolated SiO_2 precipitates distributed over a thickness of about 110 nm is formed in the reference sample [see Fig. 2(c)]. The cross sectional SSRM analysis in Fig. 3 reveals the thermally formed surface oxide and confirms that the continuous BOX layer formed at the highest He postimplantation fluence [see Fig. 2(b)] is fully insulating. Any SiO_2 precipitates that would be larger than the tip diameter[24] cannot be seen in the top Si layer. The position in depth (at 400 nm) and the thickness (about 58 nm) of the BOX layer measured by SSRM are in agreement with the XTEM result shown in Fig. 2(b). Figure 3(a) demonstrates that the upper Si/SiO_2 interface of the BOX layer is as smooth as the SiO_2/Si interface obtained by thermal surface oxidation. The inserted curve shows the resistance laterally averaged over the scanned area. The top Si layer has the same resistance as the Si substrate, whereas the measured resistance of the BOX

layer is one order of magnitude lower than the surface oxide. This may be attributed to defects such as Si rich precipitates embedded in the BOX, which is usually obtained in the SIMOX process.[25] Together with this, the apparent less uniform BOX layer shown in the SSRM image may be attributed to artifacts of the SSRM measurement, such as electrical defects or partial oxidation of the cleaved surface.

The enhancement in oxygen accumulation around D_p caused by subsequently implanted He can be explained by vacancy clusters originally generated by the oxygen implantation, which form stable complexes[6] that are precursors of nanosized He-filled bubbles.[18–20] The empty volume and the internal surfaces associated with such bubbles act as the preferential trapping centers for He and oxygen, respectively (the latter is accumulated during the annealing process).[17,19,21,22] He escapes from bubbles leaving the Si substrate at the temperature above 300 °C.[26] An increase in the He fluence may result in a higher pressure inside the bubbles, which enhances their stability against the dissolution that may occur during the temperature ramping for high temperature annealing. A longer lasting oxygen gettering effect is achieved due to the stabilization of the gettering centers. By the conventional low-fluence SIMOX process for implantation energy of 185 keV, a continuous BOX layer was never achieved at such a low oxygen fluence and small thickness. BOX layers with a thickness of 100–125 nm were formed with oxygen fluences of $(4-5)\times 10^{17}$ cm^{-2}.[25,27] Nevertheless, the BOX thickness can also be decreased by reducing the ion energy according to the so-called "energy-dose" window,[9,28,29] which, however, would decrease the thickness of the superficial Si layer.

To summarize, oxygen gettering at the damage induced by the implantation of a very low implanted oxygen fluence of 1×10^{17} cm^{-2} at 185 keV is enhanced by using a subsequent He implantation and employing additional oxygen in-diffusion from the annealing atmosphere, which benefits the SOI structure formation at D_p. In this way, an extremely thin continuous BOX layer can be formed, which is demonstrated by cross section SSRM together with XTEM.

[1] P. M. Fahey, P. B. Griffin, and J. D. Plummer, Rev. Mod. Phys. **61**, 289 (1989).
[2] K. Kyllesbech Larsen, V. Privitera, S. Coffa, F. Priolo, S. U. Campisano, and A. Carnera, Phys. Rev. Lett. **76**, 1493 (1996).
[3] R. Kalyanaraman, T. E. Haynes, V. C. Venezia, D. C. Jacobson, H.-J. Gossmann, and C. S. Rafferty, Appl. Phys. Lett. **76**, 3379 (2000).
[4] P. Pellegrino, P. Lévêque, J. Wong-Leung, C. Jagadish, and B. G. Svensson, Appl. Phys. Lett. **78**, 3442 (2001).
[5] I. Danilov, H. Boudinov, J. P. de Souza, and Yu. N. Drozdov, J. Appl. Phys. **97**, 076106 (2005).
[6] O. W. Holland, J. D. Budai, and B. Nielsen, Mater. Sci. Eng., A **253**, 240 (1998).
[7] H. Wong, N. W. Cheung, P. K. Chu, J. Liu, and J. W. Mayer, Appl. Phys. Lett. **52**, 1023 (1988).
[8] R. Kögler, A. Peeva, A. Lebedev, M. Posselt, W. Skorupa, G. Özelt, H. Hutter, and M. Behar, J. Appl. Phys. **94**, 3834 (2003).
[9] R. Kögler, X. Ou, W. Skorupa, and W. Möller, Appl. Phys. Lett. **92**, 181906 (2008).
[10] R. Kögler, A. Mücklich, L. Vines, D. Krecar, A. Kuznetsov, W. Skorupa, Nucl. Instrum. Methods Phys. Res. B **257**, 161 (2007).
[11] *SIMOX*, edited by M. J. Anc (Institution of Electrical Engineers, Stevenage, 2004).
[12] S. Bagchi and S. J. Krause, Appl. Phys. Lett. **71**, 2136 (1997).
[13] M. Tamura, M. Ishimaru, K. Hinode, K. Tokiguchi, H. Seki, and H. Mori, Jpn. J. Appl. Phys., Part 1 **45**, 7592 (2006).
[14] A. Ogura, Appl. Phys. Lett. **74**, 2188 (1999).
[15] T. Ernst, C. Tinella, C. Raynaud, and S. Cristoloveanu, Solid-State Electron. **46**, 373 (2002).
[16] N. Bresson, S. Cristoloveanu, C. Mazuré, F. Letertre, and H. Iwai, Solid-State Electron. **49**, 1522 (2005).
[17] V. Raineri, M. Saggio, and E. Rimini, J. Mater. Res. **15**, 1449 (1999).
[18] A. Van Veen, H. Schut, R. A. Hakvoort, A. Fedorov, and K. T. Westerdin, Mater. Res. Soc. Symp. Proc. **373**, 499 (1995).
[19] G. F. Cerofolini, F. Corni, S. Frabboni, C. Nobili, G. Ottaviani, and R. Tonini, Mater. Sci. Eng. R. **27**, 1 (2000).
[20] F. Corni, C. Nobili, G. Ottaviani, R. Tonini, G. Calzolari, G. F. Cerofolini, and G. Queirolo, Phys. Rev. B **56**, 7331 (1997).
[21] X. Ou, R. Kögler, A. Mücklich, W. Skorupa, W. Möller, X. Wang, J. W. Gerlach, and B. Rauschenbach, Appl. Phys. Lett. **93**, 161907 (2008).
[22] A. Ogura, Appl. Phys. Lett. **82**, 4480 (2003).
[23] J. F. Ziegler, J. P. Biersack, and U. Littmark, in *The Stopping and Ranges of Ions in Solids*, edited by J. F. Ziegler (Pergamon, New York, 1985), Vol. 1.
[24] L. Vines, R. Kögler, and A. Kuznetsov, Microelectron. Eng. **84**, 547 (2007).
[25] S. Nakashima and K. Izumi, J. Mater. Res. **8**, 523 (1993).
[26] C. C. Griffioen, J. H. Evans, P. C. de Jong, and A. van Veen, Nucl. Instrum. Methods Phys. Res. B **27**, 417 (1987).
[27] Y. Tan, B. Johnson, S. Seraphin, J. Jiao, M. J. Anc, and L. P. Allen, J. Mater. Sci.: Mater. Electron. **12**, 537 (2001).
[28] M. Chen, X. Wang, J. Chen, Y. Dong, X. Liu, Y. Yu, and X. Wang, Appl. Phys. Lett. **80**, 880 (2002).
[29] X. Wang, J. Chen, Y. Dong, M. Chen, and X. Wang, Chem. Phys. Lett. **367**, 44 (2003).